SAR-Constrained Saturation Pulse Designs Based on B0 and B1 Maps

K. Sung[1], and K. S. Nayak[1]

[1]Ming Hsieh Department of Electrical Engineering, University of Southern California, Los Angeles, CA, United States

Introduction: Saturation of longitudinal magnetization (M_z) provides the basis of T1-weighted contrast, and thus complete and uniform saturation are crucial for accurate quantitation. The performance of saturation pulses depends on homogeneities of both the static (B0) and radiofrequency (B1) magnetic fields. Many studies have shown that the rectangular RF pulse train [1] and the adiabatic B1-insensitive rotation (BIR-4) pulse [2] improve the saturation effectiveness, compared to the conventional rectangular pulse, in 1.5T and 3T cardiac imaging [3-5]. However, the pulse train has weaker immunity to B1 inhomogeneity than the BIR-4 pulse while the BIR-4 pulse has higher specific absorption rate (SAR). These costs limit their usefulness in 3T cardiac imaging where the low RF energy is highly desirable and severe B0 and B1 inhomogeneities are expected. In this work, we present a tailored pulse train design to improve the B1 variation immunity based on the previously measured B0 and B1 profiles. The measured B0 and B1 inhomogeneities guide the pulse design to produce optimal saturation effectiveness over the region of interest (ROI). Simulations and in-vivo experiments are used to evaluate the proposed saturation pulse and compare it with other current approaches.

Methods and Results: B0 and B1 profiles were measured in 8 healthy subjects (6 – 8 parallel short-axis slices for 6 subjects, and 1 short-axis slice for 2 subjects) using two GE 3T scanners. Acquisitions for B0 and B1 mapping were cardiac-gated with imaging occurring in mid-diastole, and each required one short breath-hold. The echo time difference for B0 mapping was set to 2ms (± 250Hz frequency range). The B1 scale was computed by the actual flip angle (measured value from cardiac B1+ mapping [6]) divided by the nominal flip angle (prescribed value). ROIs containing left ventricle (LV) were manually selected and their corresponding B0 and B1 values were scattered in Fig 1. A Gaussian mixture model (GMM) was used to cluster a region by performing the expectation maximization (EM) algorithm to estimate the order and parameters of GMM for a given set of observation (red line in Fig 1).

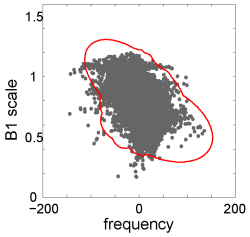

Fig 1. The B0 and B1 inhomogeneities at 3T

A tailored pulse train was designed to minimize the average residual M_z over the 2D clustered ROI for a given number of pulses (n). The train of weighted hard pulses ($\alpha_1,\cdots,\alpha_n$) was examined by an exhaustive search based on numerical Bloch simulation (ignoring T1 relaxation) where each α_i ranged from 60˚ to 240˚ with 5˚ step. The optimal weighting was chosen to generate the lowest RF energy among the group of weighting that produces within a 5% range of the minimum residual M_z. Fig 2 shows the residual M_z and relative RF energy plots as a function of n. The relative RF energy was calculated as its RF energy divided by the RF energy of the 90˚ hard pulse (512us). When n = 3 (shaded region in Fig 2), the residual M_z for the tailored pulse train **(0.060)** becomes smaller than the residual M_z for the BIR-4 pulse **(0.061)** while the relative RF energy **(4.8)** is 4.5 times lower than the BIR-4 **(21.6)**. The optimal pulse weighting was 125˚, 215˚, and 90˚ with the 8.5ms pulse duration (Fig 3). Fig 4 shows the simulated 2D profiles for the BIR-4, pulse train, and tailored pulse train with the ROI.

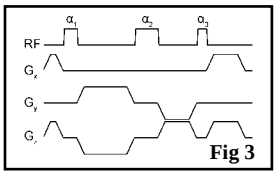

Fig 3

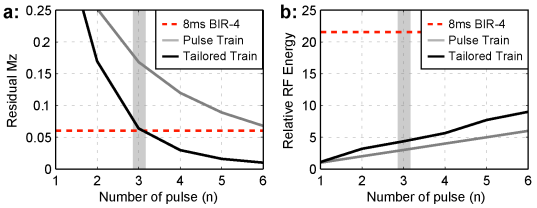

Fig 2. (a) Residual M_z and (b) relative RF energy as a function of n. The values from the BIR-4 pulse (red) are shown as the reference lines.

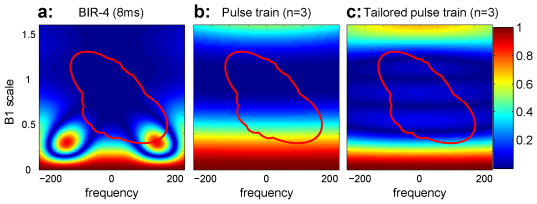

Fig 4. 2D Residual M_z profiles for (a) 8ms BIR-4 pulse, (b) pulse train (n=3), and (c) tailored pulse train (n=3).

In-vivo validation: The tailored pulse train (n=3) was evaluated by the saturation-no-recovery experiment, as previously described [4], on 3 subjects. A 2DFT FGRE acquisition with a center-out k-space trajectory was used with 10˚ flip angle. Saturation-no-recovery (SR) images and proton-density (PD) weighted images were acquired within the same breath-hold in order to normalize the equilibrium magnetization (M_o). For image analysis, the average residual M_z over LV was computed by the normalized SR images (SR/PD). Imaging parameters were: FOV = 30cm, acquisition matrix = 64×64, in-plane resolution = 4.7mm, slice thickness = 8mm, and image acquisition time = 104ms. Fig 5 shows representative PD and normalized SR images with the different saturation pulses. The residual M_z for the tailored pulse train **(0.053 ± 0.019)** was significantly smaller than those for the BIR-4 and pulse train (**0.072 ± 0.031** and **0.088 ± 0.056**, respectively; $p < 0.001$).

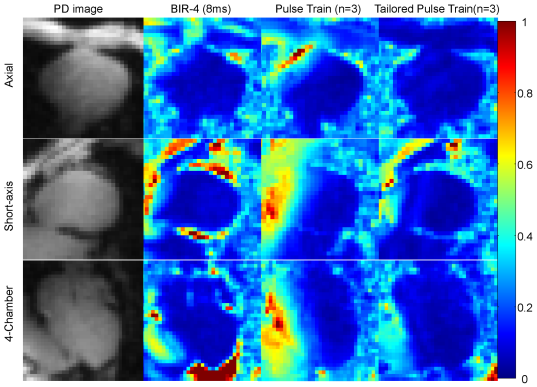

Fig 5. Representative PD and normalized SR images with different saturation pulses. The SR images of the tailored pulse train show the most complete saturation over the heart.

Discussion: The tailored pulse train demonstrated the best saturation effectiveness over the heart at 3T while requiring relative RF energy 4.5 times lower than an 8-ms BIR-4 pulse. This would reduce the possible errors in T1-weighted signals and would enable more frequent use of the saturation pulse in first-pass myocardial perfusion imaging at 3T (e.g. more slices per heartbeat). Paramagnetic contrast agents during first-pass may create an additional B0 inhomogeneity, making the B0 - B1 "foot-prints" (Fig 1) inaccurate, but we expect the proposed pulse would maintain comparable saturation effectiveness due to its B0 bandwidth (± 410Hz). The proposed pulse design can also be applied to other applications, such as quantitative abdominal imaging where accurate T1-weighted signals are required and large B0 and B1 inhomogeneities are expected.

References: [1] Oesingmann N, et al. SCMR 2004 p.489. [2] Staewen RS, et al. Investigative Radiology 1990;25:559-567. [3] Kellman P, et al. JCMR 2007;9:525-537. [4] Kim D, et al. ISMRM 2007 p.1680. [5] Kino A, et al. ISMRM 2007 p.2532. [6] Sung K. et al. ISMRM 2007 p.355.